Chemical Engineering Journal 149 (2009) 447–454

Contents lists available at ScienceDirect

Chemical Engineering Journal

journal homepage: www.elsevier.com/locate/cej

Optimisation of physical properties of γ-alumina coating microreactors used for the growth of a carbon nanofiber layer

P.A.R. Cebollada, E. Garcia-Bordejé*

Instituto de Carboquímica (C.S.I.C.), Miguel Luesma Castán 4, 50018, Zaragoza, Spain

ARTICLE INFO

Article history:
Received 30 September 2008
Received in revised form 3 February 2009
Accepted 13 February 2009

Keywords:
Microreactor
Alumina coating
Adhesion strength
Carbon nanofibers
Catalysis

ABSTRACT

This work addresses the challenging task of preparing a well-adhered and uniform coating of γ-alumina over microreactors made out of stainless steel whose composition is devoid of aluminium. The microreactors have been coated by a sol–gel method. The variation of the preparation conditions, i.e. aging time of the gel and optional step of flushing with pressurized air, rendered microreactors coated with several alumina loadings. A severe test, i.e. ultrasonic maltreatment, has been used to check the adherence of alumina layer. The optimised coating exhibited a 5–6 μm thickness, good adherence and complete coverage after ultrasound treatment. The dispersion of nickel over alumina-coated microreactor enabled to grow a layer of entangled carbon nanofibers with a thickness of 1.5–2.5 μm.

1. Introduction

The recent developments in micromachining has boosted the use of microreactors for catalytic chemical reactions. Microreactors are structured reactors with some outstanding properties. The main feature of microreactor is its high surface area to volume ratio, with values ranging from 5000 to 50,000 $m^2\ m^{-3}$, while those of conventional reactors are around 100 $m^2\ m^{-3}$. The dimensions of microreactor channels span from tens to hundreds of microns. The microscopic dimensions of the channels lend microreactors enhanced heat and mass transport properties with respect to conventional reactors.

To increase the surface area of microreactor and disperse a catalyst, it is essential to coat the microreactor with a high surface area support material. Thus, the whole preparation process of catalytic microreators needs the involvement of multidisciplinary research teams with backgrounds so different as mechanical engineering, chemistry and catalysis. Concerning the preparation of the catalytic coating, some properties are desired such as good adhesion to substrate, complete coverage and uniform thickness. A frequently used catalyst support is γ-alumina. A wide experience about coating with metal oxides layers including γ-alumina has been gained for the coating of cordierite monoliths. Cordierite monolith is also a structured reactor, which is used mainly for automotive exhaust cleaning. The adhesion strength of the wash coat to the cordierite monolith surface is a function of porosity of the cordierite surface, and the temperature history of calcination. The porosity of the ceramic monolith surface is typically 30–50% with mean pore size in the range of 3–20 μm. The larger pore sizes yield higher adhesion strengths [1]. On the other hand, stainless steel microreactors do not posses the macropores to enhance coating adhesion. Thus, the main challenge is achieving a good adhesion to the non-porous microreactor wall.

Wall-coated microreactors have been manufactured following similar washcoating technique as for cordierite monoliths [2–6]. To coat the microreactors both physical and chemical methods have been employed. Sputtering is one example of the former and sol–gel of the later. Generally, chemical methods are preferred to increase surface area and to lower deposition costs. Some researchers, prior to deposition of sols, have performed thermal oxidation of aluminum rich steel to create a porous Al_2O_3 layer, which enhances the wash coat adhesion on microchannels [7,8]. This is mainly due to the segregation of a whisker-like alumina layer after thermal treatment, which increases the adherence of catalyst layers [9]. Anodic oxidation of alumina [10] and silicon [11] has also been used to create porosity on the surface of microchannels. In these systems, the adhesion of the wash coat is determined by its ability to branch into the pore space through capillary forces and adhere mechanically after the films have been calcined. Accordingly, alumina-bearing metallic monoliths, as e.g. ferritic alloys (FeCrAlloy, Khantal, etc.), are preferred for the subsequent coating of catalyst. However, the aluminium content of alloys such as FeCrAlloy has negative implications with regard to the technique of laser welding, which is a technique commonly used for joining parts of microreactor [6]. In contrast, microreactor platelets made out of stainless steel without Al content can be tightly sealed by laser welding. Thus, the coating of microreactor substrates with a composition devoid of aluminium is challenging because it is not possible to segregate an alumina

* Corresponding author. Tel.: +34 976733977; fax: +34 976733318.
E-mail address: jegarcia@carbon.icb.csic.es (E. Garcia-Bordejé).

1385-8947/$ – see front matter © 2009 Elsevier B.V. All rights reserved.
doi:10.1016/j.cej.2009.02.016

layer to improve adherence. So far, the literature dealing with this subject is scarce [6].

Herein, we have tackled the coating with γ-alumina of microreactor platelets made out of stainless steel devoid of aluminium. We have used a sol–gel precursor to coat the monoliths and we have varied several parameters such as the pre-treatment of the support, the alumina loadings, i.e. alumina thickness, and we have studied their impact on the adhesion and morphology of the coating. Finally, Ni catalyst has been dispersed on the optimised γ-alumina microreactor coated with alumina and the catalytic microreactor has been used for the decomposition of methane. This resulted in a microreactor coated with an entangled layer of carbon nanofibers, which can be used as catalyst itself or as catalyst support and will be studied in detail in future works.

2. Experimental

The microreactor platelets were supplied by Institut für Mikrotechnik Mainz GmbH. At the bottom of Fig. 1, it is shown a microreactor platelet (14 mm × 52 mm) made out of stainless steel 1.4841. At the top, it is displayed a preliminary platelet made out of the same material. These preliminary platelets (10 mm × 10 mm) have similar channels dimensions as the microreactor platelet and they have been used for the optimisation of the coating in this work. The as-received preliminary plate is shown at the top right-hand side. At the top left-hand side, the preliminary plate after thermal treatment is displayed. The thermal treatment consisted in heating the as received microreactor in an oven at 800 °C under static air for two hours. The microreactor channels have rounded corners and their dimensions are 285 μm height and 430 μm width. The composition of the platelets determined by SEM-EDS consists mainly of Fe, Ni and Cr (Table 1).

2.1. Coating deposition

Prior to coating the microreactors, they were thoroughly rinsed with acetone. The method used to coat the microreactors is a wet chemical sol–gel method. A sol is prepared from pseudoboehmite (AlOOH, Pural from Sasol), urea and 0.3 M nitric acid with a weight ratio of 2:1:5. Likewise, a stable sol is formed. Two kinds of sols were prepared with different curing times, namely 1 h and 72 h, under stirring in an open beaker. Every channel of the microreactor platelets was filled using a syringe and assisted by the capillary forces exerted by the microchannel walls. M1 and M72 denote the microreactors coated with the sol cured during 1 h and 72 h, respectively. Some microreactores, after filling the microchannels with the two sols, were also flushed with pressurized air to remove part of the sol. These are denoted as M1F and M72F. The monoliths coated with the sol were allowed to dry at room temperature during two days. Subsequently, the coated microreactors were calcined in air flow up to 873 K with a ramp of 3 K/min and a dwell time of 1 h to obtain an γ-alumina wash coating. From the weight of the microreactor platelet before and after the coating, the alumina loading was calculated.

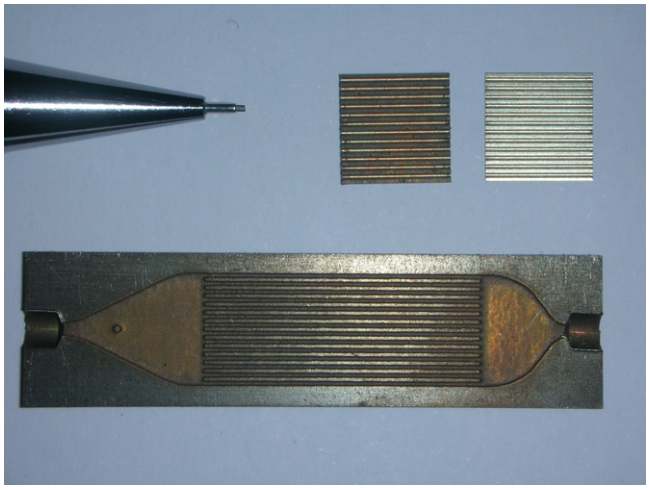

Fig. 1. Bottom: Microreactors platelet used for gas phase reaction microfabricated by IMM; Top right: preliminary platelet as-received; Top left: preliminary platelet after thermal treatment in static air at 1073 K. This latter has the same channel size than the microreactor at the bottom and it is used for coating experiments.

Table 1
EDS analysis of the top-most surface of plates.

	As-received plate	Calcined plate	
	wt.%	wt.%	wt.% normalized without O
Fe	69.8	60.29	68.79
Cr	17.77	17.02	19.42
O	0	12.37	–
Ni	11.39	8.21	9.37
S	0.83	1.09	1.24
Si	0.22	1.03	1.17

2.2. Catalytic test in the decomposition of methane to grow CNF layer

Nickel was deposited by equilibrium adsorption from a pH-neutral nickel solution. Briefly, 29 g $Ni(NO_3)_2{\cdot}6H_2O$ (pure, Sigma–Aldrich), 80 g NH_4NO_3 (pure, Sigma–Aldrich) and 4 ml ammonia solution (25%) were mixed in a 1 l bottle. The microreactor samples were kept overnight in this solution. Then the microreactors were rinsed thoroughly with deionised water, followed by drying first at room temperature overnight and later at 373 K for 1 h. Subsequently, the Ni-impregnated Al_2O_3-coated microreactors were calcined in flowing nitrogen (1 K/min) up to 873 K followed by a 2 h dwell time. The Ni content in the monoliths was measured by inductive coupled plasma-optical emission spectroscopy (ICP-OES).

The Ni/alumina-coated microreactor was tested in the decomposition of CH_4 to produce a layer of carbon nanofibers. The reaction was conducted in a horizontal quartz reactor. First, the reduction of the calcined catalyst was carried out in 100 ml/min of a mixture H_2:N_2 (50%) at 823 K for 1 h (heating rate 10 K/min). The reactor was then heated (10 K/min) to 873 K. Once the temperature was reached, 100 ml/min of CH_4:H_2 (80:20 ml/min) gas mixture was admitted and the reaction was maintained during 2 h.

2.3. Characterization techniques

SEM analysis was carried out with a microscope SEM EDX Hitachi S-3400 N with variable pressure up to 270 Pa and with an analyzer EDX Röntec XFlash de Si(Li). The images were obtained both from the secondary and backscattered electrons signal. The alumina thickness was measure from backscattered SEM photomicrographs of lateral view of a microreactor channel.

The adhesion was checked by the weigh loss after treatment in an ultrasonic apparatus (frequency 40 KHz) with a generator power of 100 W. The microreactor sample was immersed in a petroleum ether bath and was kept for different durations. Subsequently, the sample was dried, weighted and characterised.

Nitrogen adsorption–desorption isotherms were measured at 77 K using a Micromeritics ASAP 2020. Total surface area and pore volumes were determined using the BET (Brunauer–Emmett–Teller) equation and the single point method, respectively. Mesopore surface area was determined by *t*-plot method. The surface area of the alumina coated microreactors was

expressed in terms of an enhancement factor *F*, defined by the ratio of the measured BET surface area (m^2) to the geometrical surface area of the microreactor channels (m^2) as defined in reference [12]. Thus, a perfectly pore free and flat coating would have a surface enhancement factor of 1 m^2/m^2.

3. Results

3.1. Modification of microreactor surface by thermal pre-treatment

Fig. 2a–c shows the top view of a channel of microreactors as-received, after thermal treatment, and after coating with alumina. After coating with alumina (Fig. 2c) the image becomes blurred because alumina is less electron-conductive. After the thermal treatment (Fig. 2b), it is observed that the surface has a grainy fine structure with higher roughness than the original microreactor. This is also apparent in the cross-view of a channel where drop-like features are visible in the top-most surface (Fig. 3b), while the profile of the original channel is sharp (Fig. 3a). The top surface was analysed by EDS and the results are displayed in Table 1. After thermal treatment, oxygen is detected on the surface suggesting the presence of metal oxides. To check for the possible segregation of metals, the relative percentage of metals disregarding oxygen contribution was calculated, which is shown in last column of Table 1. The comparison of these data with those of as-received plate (first column) reveals that the surface is enriched in Si and Cr. Thus, oxides of Cr and Si segregated to the surface after thermal treatment. The increase is more relevant for Si, which experiences a 5-fold increase on the surface. The segregation of these metal oxides to the surface can account for the grainy features in SEM pictures (Fig. 3b). The roughness created on the microreactor by thermal treatment must help to increase the adhesion of deposited alumina layer.

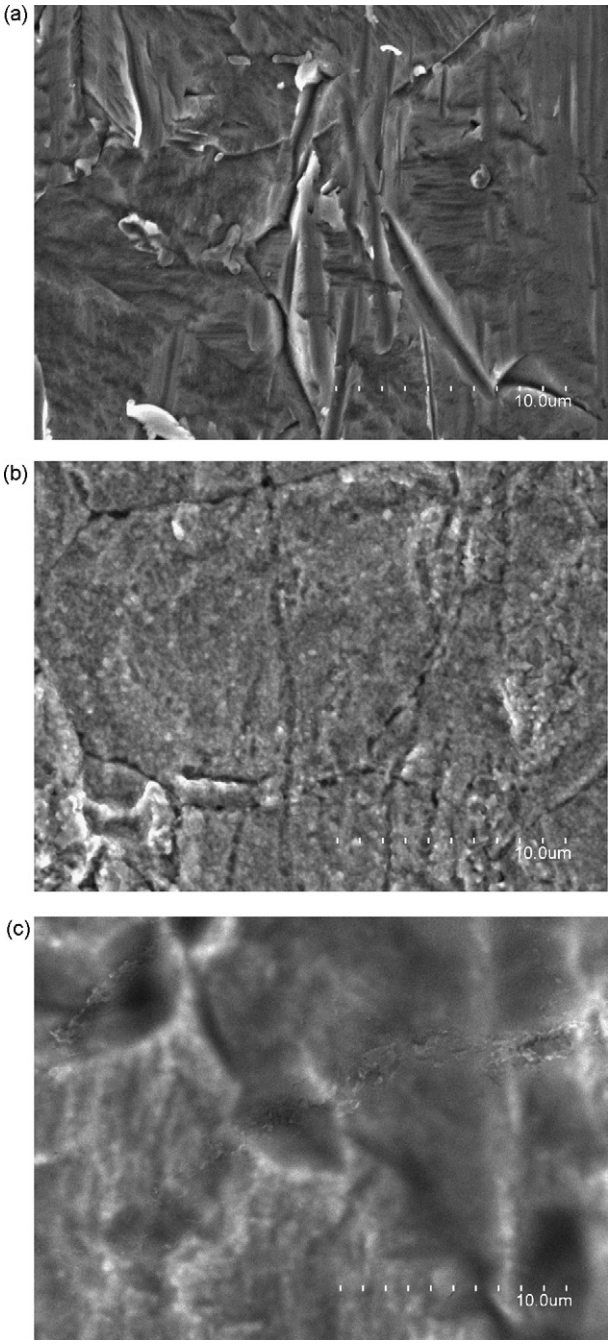

Fig. 2. Top view SEM image of microchanel of: (a) as-received platelet; (b) after thermal treatment; (c) after coating with γ-alumina.

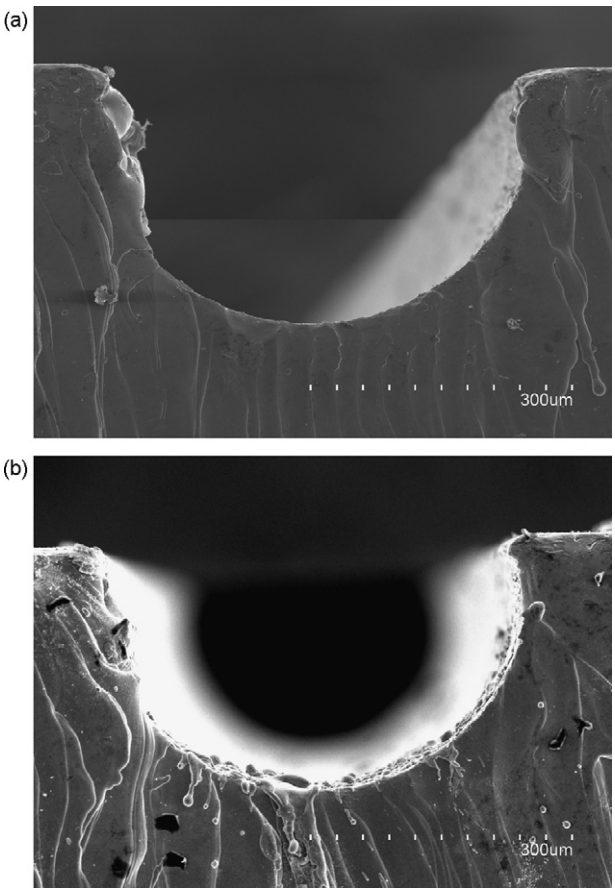

Fig. 3. Cross section of a microchannel: (a) as received; (b) after thermal treatment.

3.2. Characterisation of the microreactors after coating with several alumina loadings

For comparison of microreactor morphology after coating with different alumina loadings, the microractors were characterised by SEM microscopy. Fig. 4 shows SEM top view image of the microreactor calcined (Fig. 4a), microreactor M1 with ~0.3 wt.% alumina (Fig. 4b) and microreactor M1F with ~0.1 wt.% alumina (Fig. 4c). Fig. 5a–c displays lateral view of the same microreactors. SEM images of M72 and M72F, which are not shown here

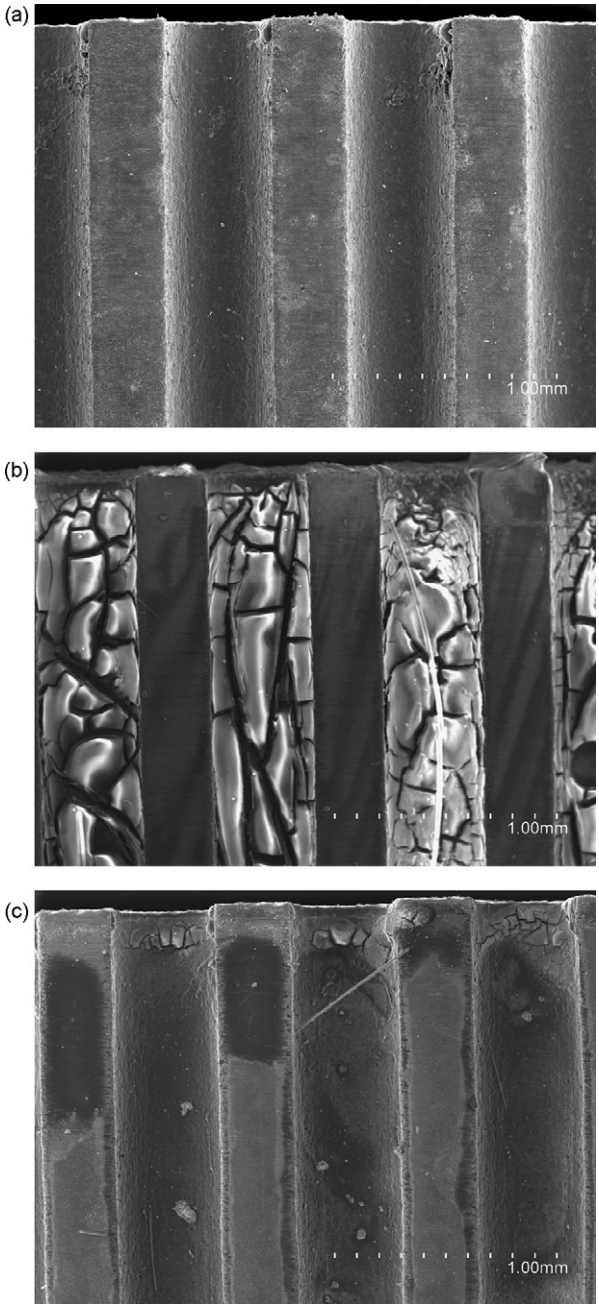

Fig. 4. General top view SEM image of several microchannels of the microreactor: (a) as-received; (b) M1, microreactor coated with ~0.3 wt.% of alumina; (c) M1F, microreactor coated with ~0.1 wt.% alumina.

for brevity, are comparable to images of M1 and M1F, respectively.

It is apparent that in sample M1 numerous cracks are formed after calcination (Figs. 4b and 5b). However, in sample M1F, the surface is more uniform and only some small cracks are observed at the extreme part of the microchannel (Fig. 4c). This is attributed to the accumulation of alumina sol at the microchannel extremes because flushing is more effective at the centre than at the border.

3.3. Testing of the alumina coating adherence by ultrasonication

The adherence of coatings is usually checked in the literature by a harsh treatment in ultrasonic bath. Fig. 6 shows the weight loss as a function of the time of treatment in ultrasonic bath for the microreactors coated with several alumina percentages. The major weight loss occurs in the first 30 min after ultrasonication. After this time, the weight remains constant for the microreactors with the lowest γ-alumina loadings, i.e. M1F and M72F, while for M1 and M72 the weight continues decaying slowly, almost until the end of the experiment. At this point, around a 60 wt.% of alumina has been lost in M1 and M72, whereas only ca. 40 wt.% reduction of alumina weight has taken place in microreactors M1F and M2F.

We further characterise the morphology of the coating after ultrasonic maltreatment by scanning electron microscopy. Fig. 7 shows the morphology of two microreactors, i.e. M1 (Fig. 7a)

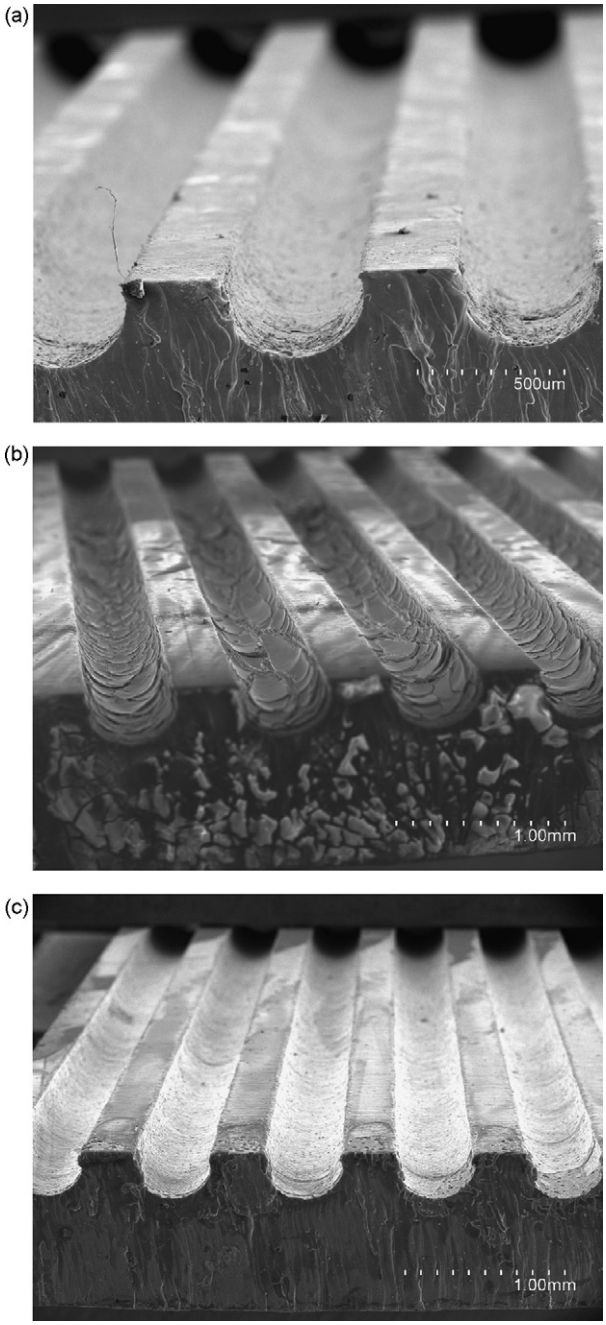

Fig. 5. lateral view SEM image of several microchannels of the microreactor: (a) as-received; (b) M1, microreactor coated with ~0.3 wt.% of alumina; (c) M1F, microreactor coated with ~0.1 wt.% alumina (backscattered image where the darkest contrast is alumina coating).

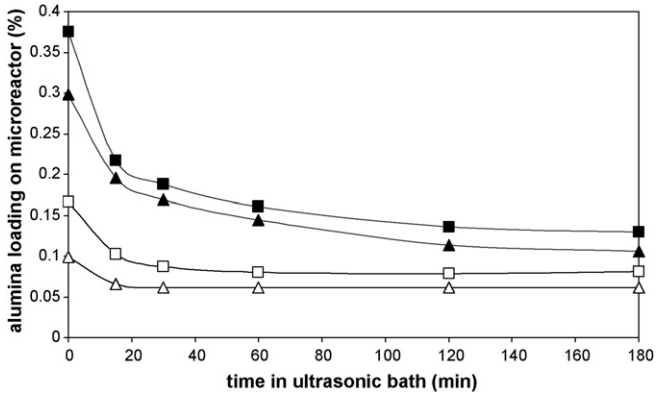

Fig. 6. Weight loss as a function of time of ultrasonic treatment for microreactors with different alumina loading. ratio (ml/g): (▲) M1, (△) M1F, (■) M72, (□) M72F.

and M1F (Fig. 7b), after 30 min in ultrasonic bath. M1 microreactor has undergone an extensive alumina peeling-off. This is more pronouncedly at the extremes of microreactor, possibly because mechanical stresses during ultrasonic treatment are stronger in this part. This peeling-off is favoured by the cracks observed prior to ultrasonication (Fig. 5b). Conversely, the surface of M1F (Fig. 7b) exhibits a uniform surface without apparent damage.

The microreactors were also characterised after 180 min of ultrasonic treatment. Figs. 8 and 9 display SEM images of these microreactors. Concerning sample M1, if we compare Fig. 8a with Fig. 7a, it is apparent that after a longer ultrasonic treatment,

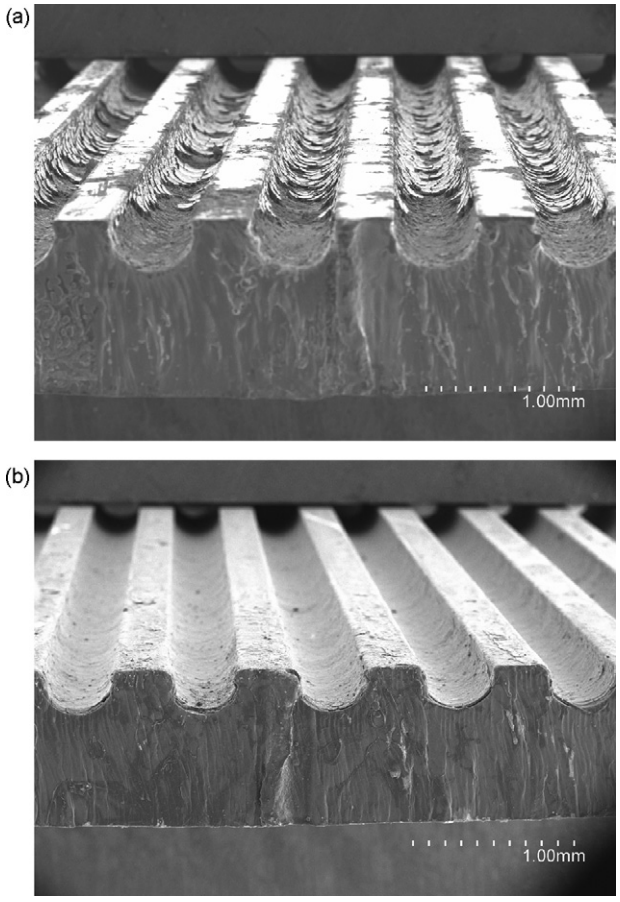

Fig. 7. SEM images of samples M1 (a) and sample M1F (b) after 30 min in ultrasonic bath.

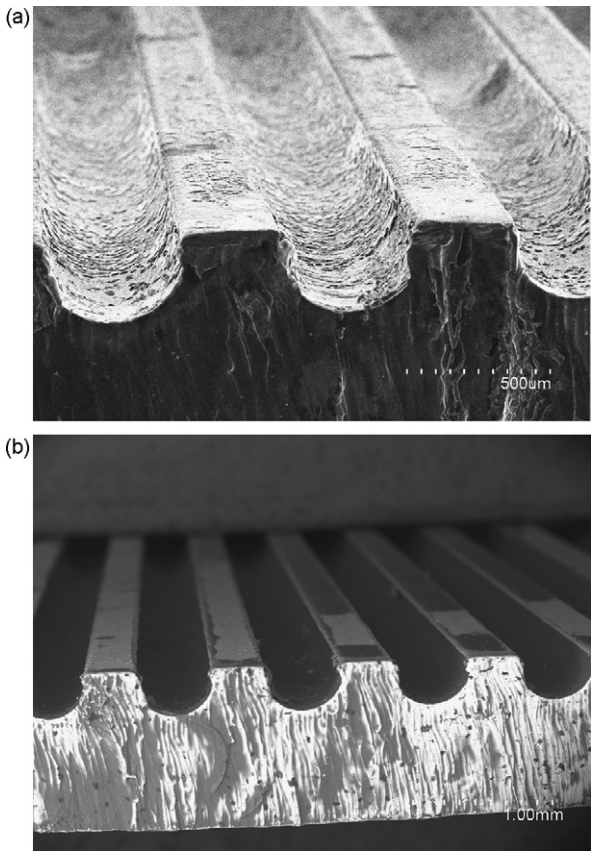

Fig. 8. SEM images of samples M1 (a) and sample M1F (b) after 180 min in ultrasonic bath. (b) is a backscattered SEM image where the darkest contrast is the alumina coating.

i.e. 180 min, an almost complete peeling-off occurred. In fact, 60 wt.% of the alumina coating was removed at the end of ultrasonic treatment. The higher magnification image (Fig. 9a) shows some sparse alumina patches, rendering a irregular surface. These remaining patches are very well anchored because they withstood the severe ultrasonic maltreatment. On the contrary, for microreactor M1F (Fig. 9b) the surface of microchannel is more regular, exhibiting the roughness characteristic from the microreactor after thermal treatment. Thus, the alumina coating adapts to this roughness without any apparent alumina patches. The lower weight loss after sonication for microreactors M1F and M72F is attributed to the better anchorage and the almost total absence of cracks. Moreover, the surface is completely covered by alumina, as observed in backscattered image of microreactor M1F (Fig. 8b). The darkest contrast corresponds to the alumina coating.

3.4. Alumina thickness and porosity after sonication

The theoretical thicknesses before and after sonication are listed in Table 2. This thickness has been calculated from alumina weight assuming a uniform coverage of the microchannel walls and using a density for alumina of 0.9 g/cc. The assumption of uniform coverage is more realistic in the case of samples with lower alumina loading M1F and M72F as observed in Fig. 9b.

To have an indication of actual alumina thickness we recorded backscattered SEM images at the border of microchannels. Figs. 10 and 11 show backscattered SEM images for ultrasonicated microreactors M72F and M1F, respectively. In the case of M72F, the alumina coating thickness is quite uniform with an average thickness of

Table 2
Weight losses after ultrasound treatment for 180 min of microreactors coated with several alumina loadings and theoretical γ-alumina thicknesses.

Microreactor	Initial Al_2O_3 loading (%)	Al_2O_3 loading after ultrasound (%)	Al_2O_3 loss after ultrasound (%)	Initial Al_2O_3 theoretical thickness (μm)	Final Al_2O_3 theoretical thickness (μm)
M72	0.375	0.130	65	29.5	10.2
M1	0.298	0.106	64	23.3	8.3
M72F	0.167	0.081	43	15.6	6.4
M1F	0.099	0.061	38	7.78	4.8

8 μm in the border of microchannel. This agrees acceptably with the calculated theoretical thickness of 6.4 μm. Moreover, a slightly higher alumina loading could be envisaged at the extremes than in center of microchannels because of border effects during the procedure of flushing the alumina sol. In the case of microreactor M1F, we found more dispersion in the thickness, which was frequently between 4 and 7 μm but in some cases reached up to 14 μm (Fig. 11a). These values are also slighly larger than the theoretical thickness of 4.8 μm, which is attributed to the uneven distribution of sol along the microchannel during flushing.

Table 3 displays the values of the textural characterisation by N_2 physisorption. The γ-alumina is mesoporous with an average pore size of 3.6 nm. The resulting alumina coated microreactor M72F exhibits a surface enhancement factor (SEF) of 1350 m^2/m^2. The SEF is calculates as the ratio between the surface area (S_{BET}) of the microreactor to the geometric area of the platelet. Thus, the washcoated microreactor exposes an 1350 times larger surface for the catalytic reaction. The value of SEF calculated here is comparable or slightly larger than those reported in the literature [7,12].

3.5. Catalytic test of microreactor in the decomposition of CH_4 to produce a layer of entangled CNF

Ni catalyst was dispersed on the microreactor M72F after ultrasonic treatment as explained in experimental section. This method rendered Ni particles very well dispersed in a previous work [13]. After calcination, the Ni loading on alumina-coated microreactor was determined to be 11 wt.% with respect to alumina weight by ICP-OES. In the condition of reaction used, the yield of CNFs was 75 wt.% with respect to alumina weight. Some SEM images of the microreactor after the CNF grow are shown in Fig. 12. Carbon nanofibers are entangled and with diameters uniform and smaller than 50 nm. The CNF layer has thicknesses ranging from 1.3 to 2.5 μm. Fig. 13 shows the microreactor platelets as-received, coated with alumina and after CNF growth. The black colour due to CNFs is clearly observed on the microchannels (Fig. 13c). The study of the conditions of CNF growth, the characterisation of the microreactors coated with CNFs and its catalytic testing will be the subject of future work.

In the conditions of CNF growth used herein, the presence of the alumina coating is essential for the growth of CNFs. In the lit-

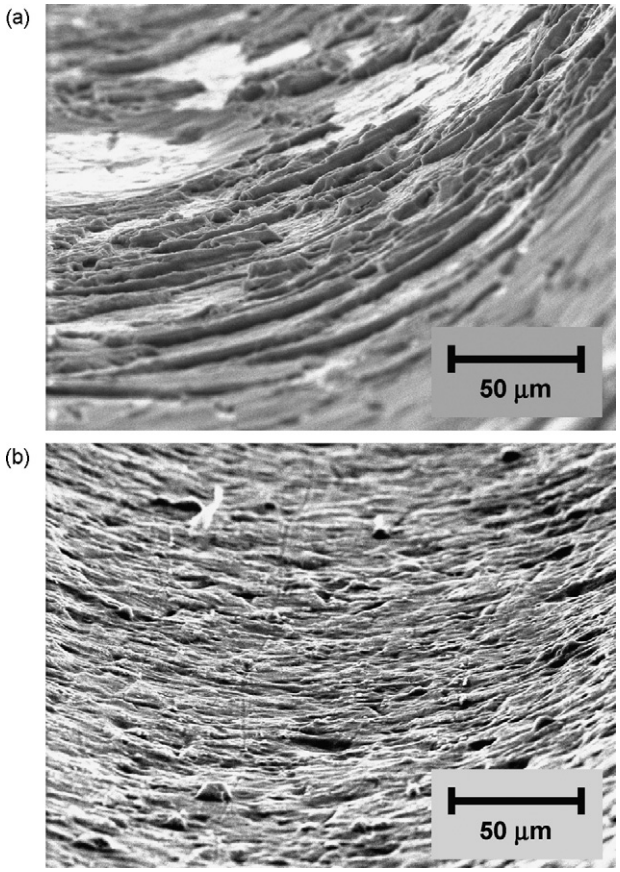

Fig. 9. High-magnification SEM images of microreactors M1 (a) and M1F (b) after 180 min in ultrasonic bath. It is possible to observe details of the alumina coating microchannels wall.

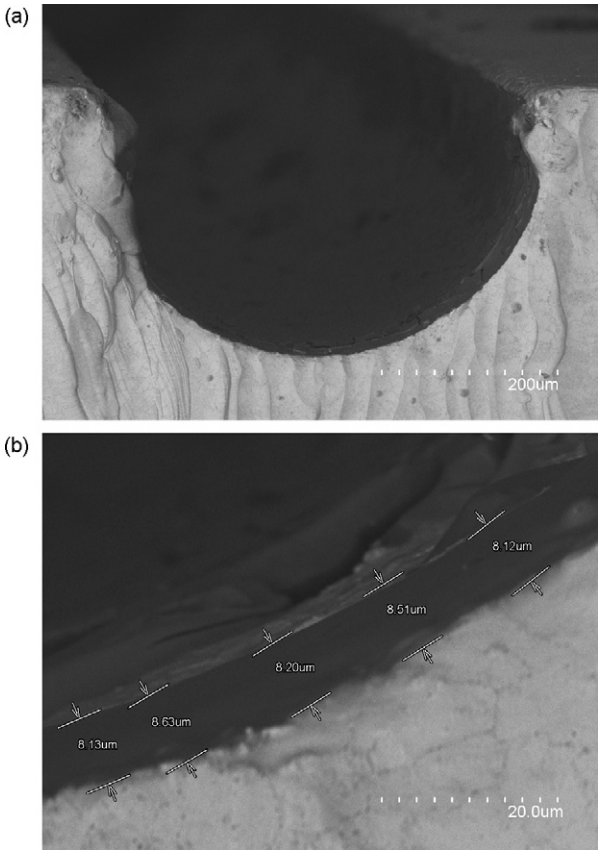

Fig. 10. SEM image with backscattered electrons of microreactor M72F. (a) image of a microchannel, (b) detail of a microchannel border. The darkest contrast corresponds to alumina coating.

Table 3
Textural characterization of alumina coating by N_2 physisorption.

	S_{BET} (m^2/g)	$S_{mesopores}$ (m^2/g)	Surface enhancement factor (SEF) (m^2/m^2)	Pore volume (cm^3/g)	Average pore diameter (nm)
Al_2O_3 coating	238	234	~1300	0.26	3.6

erature [14,15], CNF have been grown over metal substrates since metals contained in the stainless steel (Ni, Fe) can catalyse CH_4 decomposition. We also attempted to grow CNF over microreactor without alumina coating but CNF yield was negligible. By visual examination of microreactor, only some small areas of apparent CNF growth were observed (black colour). We examined one of these areas by SEM (Fig. 14). The CNFs are sparse and with larger diameter than in the alumina-coated microreactor. We deem that it could be possible to achieve higher CNF yield on alumina-free microreactor by using a gas more reactive than CH_4. Nevertheless, the direct growth of CNF on stainless steel supports usually produced nanocarbon materials of heterogeneous morphology and size, ranging from amorphous carbon to different types of nanofibers [14,15]. This is due to the poorly defined stainless steel surface in terms of grain sizes and local composition. Thus, the pre-coating of a tailored CNF-growth catalyst on stainless steel substrate enables more control over morphology and size of CNFs and, in turn, over uniformity of CNF layer.

Several works have reported the gowth of a carbon nonotube (CNT) layer on silica microreactors by a floating catalyst method. In one of these works [16], Pd was supported on CNT/microreactor leading to unprecedented selectivities in the hydrogenation of cinnamaldehyde. In other work [17], a layer of aligned MWCNT were grown also on silica microreactors and, after Pt nanoparticles deposition, it was tested in the hydrosilylation of an olefin. It was found that the presence of aligned nanotubes significantly enhances the catalytic reaction and extends the catalyst lifetime as compared with conventional microreactors using a Pt metal film or Pt nanoparticles directly deposited on the channel walls. To our knowledge, it has not been reported so far the growth of a CNT or

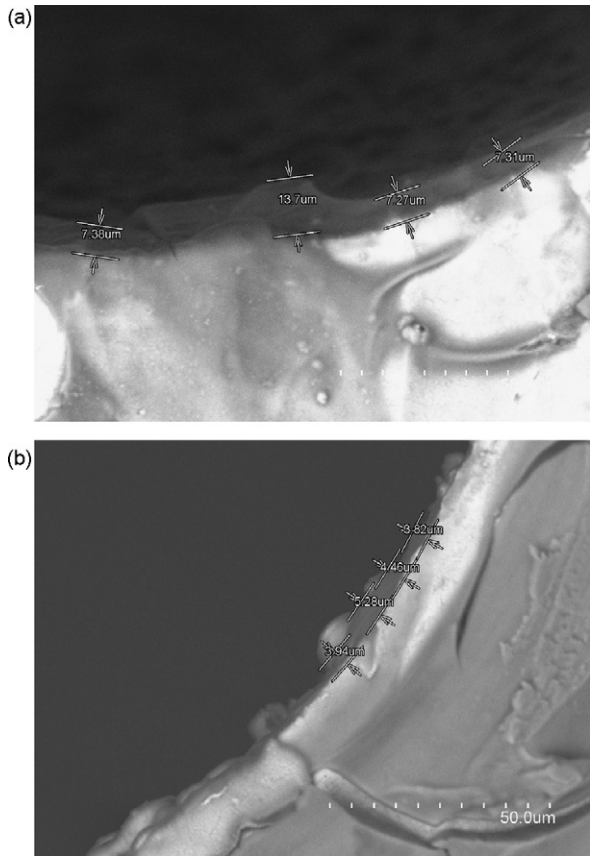

Fig. 11. SEM images with backscattered electrons recorded at the border of a microchannel in microreactor M1F in two different locations.

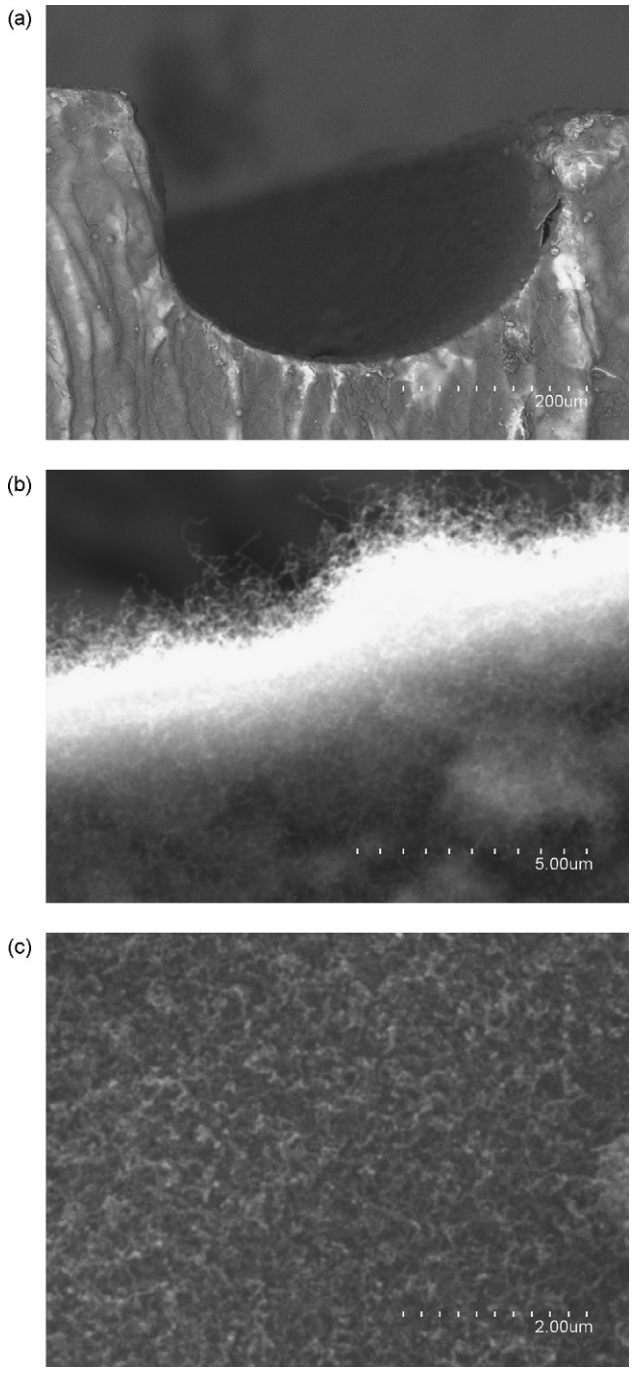

Fig. 12. Microreactor M72F after CNF grow. (a) detail of a microchannel; (b) cross section of CNF layer; (c) tow view of a microchannel coated with nanofibers.

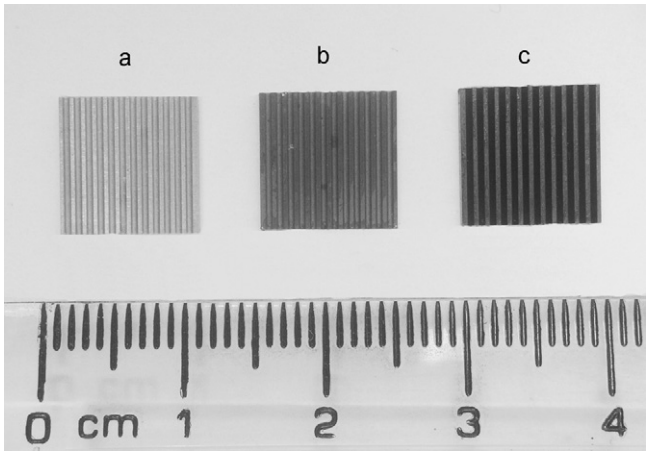

Fig. 13. Visual observation of microreactor platelets corresponding to several steps. (a) as-received platelet, (b) platelet after alumina coating, (c) platelet after CNF growth.

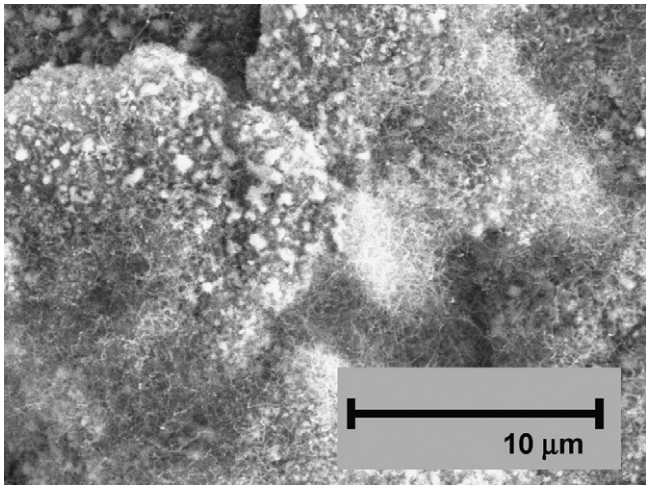

Fig. 14. CNF grown on microreactor without alumina coating. There are places (top left) where there is no CNF growth. In general the CNFs are of larger diameter and less dense than in Fig. 12c.

CNF layer on a stainless steel microreactor. This would open new perspectives for the application of stainless steel microreactors to catalyzed reactions.

4. Conclusions

The thermal pre-treatment of the microreactor creates a surface with a grainy morphology, which is beneficial for the adhesion of the alumina coating. The formation of this morphology is due to the segregation to the surface of silica and chromium oxides. The microreactors coated with the highest alumina loading resulted in the formation of microcracks during the calcination step. This led to a bad adhesion of the coating and the coating is lost continuously during the whole duration of ultrasound treatment, i.e. 180 min. On the other hand, microreactor coated with the lowest alumina loadings lost some badly adhered coating within the first 20 min of ultrasound treatment and they remain stable for prolonged times. After ultrasound treatment, a stable alumina coating covers the surface of microchannels completely. Therefore, this sol–gel approach enabled to adhere a coating of γ-alumina strongly to a microreactor platelet made out of stainless steel without aluminium content. The alumina coating has average thickness of 5–6 μm. This alumina coating increased the surface area of the microreactor by a factor of ~1300.

After dispersing Ni catalyst on the alumina coating of ultrasonicated microreactors, we have grown carbon nanofibers by thermocatalytic decomposition of CH_4. The CNFs have diameters smaller than 50 nm and they formed an entangled layer covering completely the channels of microreactor. The CNF layer has a thickness between 1.3 and 2.5 μm. The complete alumina coverage after ultrasonic treatment is deemed essential for the growth of a uniform CNF layer from CH_4 decomposition since microreactors without previous alumina coating resulted in negligible CNF yield. Both the alumina-coated microreactors and CNF-coated microreactors can find application in catalytic reactions where the capacities of microreactors can be fully exploited, as e.g. for H_2 generation on board of a vehicle where fast heating-up and cooling-down is needed.

Acknowledgements

I. Tacchini is acknowledged by the helpful discussions and assistance in the interpretation of SEM images. We are also indebted to CSIC for the financial support through a “Proyecto Intramural” 200780/010.

References

[1] A. Cybulski, J.A. Moulijn, Catalysis Reviews-Science and Engineering 36 (1994) 179.
[2] I. Aartun, T. Gjervan, H. Venvik, O. Gorke, P. Pfeifer, M. Fathi, A. Holmen, K. Schubert, Chemical Engineering Journal 101 (2004) 93.
[3] A. Stefanescu, A.C. van Veen, C. Mirodatos, J.C. Beziat, E. Duval-Brunel, Catalysis Today 125 (2007) 16.
[4] J. Bravo, A. Karim, T. Conant, G.P. Lopez, A. Datye, Chemical Engineering Journal 101 (2004) 113.
[5] M. Valentini, G. Groppi, C. Cristiani, M. Levi, E. Tronconi, P. Forzatti, Catalysis Today 69 (2001) 307.
[6] R. Zapf, G. Kolb, H. Pennemann, V. Hessel, Chemical Engineering & Technology 29 (2006) 1509.
[7] K. Haas-Santo, M. Fichtner, K. Schubert, Applied Catalysis A: General 220 (2001) 79.
[8] M.F.M. Zwinkels, S.G. Järås, P.G. Menon, K.I. Åsen, Journal of Materials Science 31 (1996) 6345.
[9] P. Avila, M. Montes, E.E. Miro, Chemical Engineering Journal 109 (2005) 11.
[10] G. Wiessmeier, D. Honicke, Journal of Micromechanics and Microengineering 6 (1996) 285.
[11] M.W. Losey, R.J. Jackman, S.L. Firebaugh, M.A. Schmidt, K.F. Jensen, Journal of Microelectromechanical Systems 11 (2002) 709.
[12] A. Stefanescu, A.C. van Veen, E. Duval-Brunel, C. Mirodatos, Chemical Engineering Science 62 (2007) 5092.
[13] E. Garcia-Bordeje, I. Kvande, D. Chen, M. Ronning, Carbon 45 (2007) 1828.
[14] P. Tribolet, L. Kiwi-Minsker, Catalysis Today 102 (2005) 15.
[15] R.L. Vander Wal, L.J. Hall, Carbon 41 (2003) 659.
[16] I. Janowska, G. Wine, M.J. Ledoux, C. Pham-Huu, Journal of Molecular Catalysis A-Chemical 267 (2007) 92.
[17] N. Ishigami, H. Ago, Y. Motoyama, M. Takasaki, M. Shinagawa, K. Takahashi, T. Ikuta, M. Tsuji, Chemical Communications 16 (2007) 1626.